

MODELING DEVELOPMENTAL, MOLECULAR, AND BEHAVIORAL EFFECTS  
OF AN APOLIPOPROTEIN-E4 FRAGMENT ON THE EMBRYOGENESIS OF  
ZEBRAFISH

by

Madyson McCarthy



A thesis

submitted in partial fulfillment

of the requirements for the degree of

Master of Science in Biology

Boise State University

May 2022

© 2022

Madyson McCarthy

ALL RIGHTS RESERVED

BOISE STATE UNIVERSITY GRADUATE COLLEGE

**DEFENSE COMMITTEE AND FINAL READING APPROVALS**

of the thesis submitted by

Madyson McCarthy

Thesis Title: Modeling Developmental, Molecular, and Behavioral Effects of an Apolipoprotein-E4 (ApoE4) Fragment on the Embryogenesis of Zebrafish (*Danio rerio*)

Date of Final Oral Examination: 15 March 2022

The following individuals read and discussed the thesis submitted by student Madyson McCarthy, and they evaluated the student's presentation and response to questions during the final oral examination. They found that the student passed the final oral examination.

Troy Rohn, Ph.D. Chair, Supervisory Committee

Julia Oxford, Ph.D. Member, Supervisory Committee

Juliette Tinker, Ph.D. Member, Supervisory Committee

The final reading approval of the thesis was granted by Troy Rohn, Ph.D., Chair of the Supervisory Committee. The thesis was approved by the Graduate College.

## DEDICATION

This thesis is dedicated to my husband, Scott, and everyone who helped me move mountains to arrive at this moment.

## ACKNOWLEDGMENTS

The number of people who rallied together to complete the hands-on research, consultation, and provide emotional support throughout the process of completing this project far outnumber the amount of space provided to recognize every one by name. Thank you to Dr. Juliette Tinker and Dr. Julia Oxford for serving on my thesis committee and providing constructive feedback throughout my project. Thank you to the Oxford Lab for welcoming me into your space to watch, learn, and grow alongside your team. Specifically, thank you to Dr. Makenna Hardy, who provided the bulk of my hands-on training and made the graduate school process that much easier. Thank you to Stephanie Tuft, for managing an efficient laboratory space and for building an environment where the laboratory team felt more like family. Another large thank you to Dr. Julia Oxford for the conceptual support you have provided throughout my time here and for the encouragement to keep pursuing something more. Lynn Karriem, for helping make the past few years interesting. From the Rohn lab, thank you to everyone who worked with me along the way: Amelia Cogan, Erica Stewart, Saylor Leising, Katie Matteo, and Noail Isho. The contributions made to this thesis were valued just as much as your companionship along the way. Last, but not least, Dr. Troy Rohn. Thank you for your support over the past 3 difficult years. I am grateful to have had the opportunity to work in your lab and receive a high level of support not only as a researcher, but as a human being.

## ABSTRACT

Although the increased risk of developing sporadic Alzheimer's disease (AD) associated with the inheritance of the apolipoprotein E4 (*APOE4*) allele is well characterized, the molecular underpinnings of how ApoE4 imparts risk remains unknown. Enhanced proteolysis of the ApoE4 protein with a toxic-gain of function has been suggested and a 17 kDa amino-terminal ApoE4 fragment (nApoE4<sub>1-151</sub>) has been identified in post-mortem human AD frontal cortex sections. Recently, we demonstrated *in vitro*, exogenous treatment of nApoE4<sub>1-151</sub> in BV2 microglial cells leads to uptake, trafficking to the nucleus and increased expression of genes associated with cell toxicity and inflammation. In the present study, we extend these findings to zebrafish (*Danio rerio*), which is an emerging *in vivo* model system to study AD. Exogenous treatment of nApoE4<sub>1-151</sub> to 24-hour post-fertilization for 24 hours resulted in significant mortality. In addition, developmental abnormalities were observed following exogenous treatment with nApoE4<sub>1-151</sub> including improper folding of the hindbrain, delay in ear development, deformed yolk sac, enlarged cardiac cavity, and significantly lower heart rates. Decreased presence of pigmentation was noted for nApoE4<sub>1-151</sub> treated fish compared with controls. Touch-evoked responses to stimuli were negatively impacted by treatment with nApoE4<sub>1-151</sub>. A similar nApoE3<sub>1-151</sub> fragment that differs by a single amino acid change (C>R) at position 112 had no effects on these parameters under identical treatment conditions. Additionally, triple-labeling confocal microscopy not only confirmed the nuclear localization of the nApoE4<sub>1-151</sub> fragment within neuronal populations following

exogenous treatment, but also identified the presence of tau tangle pathology, one of the hallmark features of AD. Collectively, these *in vivo* data demonstrating toxicity as well as sublethal effects on organ and tissue development support a novel pathophysiological function of this AD associated-risk factor.

## TABLE OF CONTENTS

DEDICATION.....	iv
ACKNOWLEDGMENTS.....	v
ABSTRACT .....	vi
LIST OF TABLES.....	xi
LIST OF FIGURES .....	xii
LIST OF ABBREVIATIONS.....	xiii
CHAPTER ONE: INTRODUCTION.....	1
Alzheimer’s Disease .....	1
ApoE4 Structure and Function.....	1
Zebrafish as a Model for Alzheimer’s Disease.....	4
Hypothesis.....	5
Tables.....	7
CHAPTER TWO: MORPHOLOGICAL EFFECTS.....	8
Overview.....	8
Materials and Methods .....	9
Synthesis of nApoE <sub>1-151</sub> fragments.....	9
Zebrafish Embryo Care and Maintenance.....	9
Treatment of Embryos with exogenous ApoE <sub>1-151</sub> fragments .....	10
Live Imaging (Light Microscope).....	10



Morphological Assessments .....	11
Heart Rate Determination .....	11
Results .....	11
Embryonic Survivability.....	11
Developmental Abnormalities .....	12
Heart Rate .....	12
Conclusions .....	13
Tables .....	14
Figures.....	15
CHAPTER THREE: MOLECULAR EFFECTS .....	18
Materials and Methods .....	19
Zebrafish Homogenate Preparation and Cytotoxic Assays .....	19
Immunohistochemistry .....	20
Results .....	21
Toxicity.....	21
Pierce Lactate Dehydrogenase Assay.....	21
Caspase-3 Western Blot.....	21
Immunohistochemistry .....	22
Conclusions .....	22
Tables .....	23
Figures.....	24
CHAPTER FOUR: BEHAVIORAL EFFECTS .....	28
Overview .....	28

Materials and Methods .....	29
Tail Flick Behavioral Test.....	29
Touch Evoked Movement Response Assay .....	30
Results.....	31
Tail Flick Test Assay .....	31
Touch-Evoked Movement Response Assay .....	31
Conclusions.....	31
Figures .....	33
CHAPTER FIVE: DISCUSSION.....	35
REFERENCES .....	38

## LIST OF TABLES

Table 1.	Overview of AD associated genes in human versus zebrafish. ....	7
Table 2	Stages of Embryonic Development (Condensed from (Kimmel et al., 1995)). Stages of development were assessed by evaluating the embryos in our projects in comparison to the scale provided below. Morphological features provided in the table were then used to set a normal developmental timeline criteria for controls. ....	14
Table 3.	Antibodies used in Immunohistochemistry Experiments. ....	23

## LIST OF FIGURES

Figure 1.	Project specific developmental abnormality scale.....	15
Figure 2.	Survivability decreased in zebrafish embryos following exogenous treatment with an amino-terminal fragment of nApoE4 <sub>1-151</sub> . ....	16
Figure 3.	A sublethal concentration of nApoE4 <sub>1-151</sub> leads to morphological abnormalities in zebrafish embryos at the hatching phase. ....	17
Figure 4.	Measurements of LDH and apoptosis indicate a cytotoxic role for nApoE4 <sub>1-151</sub> (A-C). ....	24
Figure 5.	Exogenous treatment of zebrafish embryos with amino-terminal fragments of nApoE4 <sub>1-151</sub> leads to nuclear localization. (A-D).....	25
Figure 6.	Tau Pathology present after treatment with exogenous nApoE4 <sub>1-151</sub> Fragment in 48hpf zebrafish brain. (A-D).....	26
Figure 7.	Tau Pathology present after treatment with exogenous nApoE4 <sub>1-151</sub> Fragment in 72hpf zebrafish brain. (A-D).....	27
Figure 8.	TFT trials finds no difference in unstimulated muscle twitches between treatment groups (A-C). ....	33
Figure 9.	Touch-Evoked Movement Response outcomes lack significance but identify a clear decreasing trend through treatment groups. ....	34

## LIST OF ABBREVIATIONS

AD	Alzheimer's disease
PSEN 1/2	Presenilin 1 and 2
APOE	Apolipoprotein E gene
<i>APOE2/3/4</i>	Apolipoprotein allele E2/E3/E4
NFT	Neurofibrillary Tangles
APP	Amyloid precursor protein
A $\beta$	Beta amyloid
kDa	Kilo Dalton
HPF	Hours post-fertilization
DPF	Days post-fertilization
MMP	Matrix metalloproteinases
LDL	Low-density lipoprotein
LDLR	Low-density lipoprotein receptor
LRP	Low-density
PBT	Phosphate buffered saline Tween 20
MAPT	Microtubule associated protein tau



## CHAPTER ONE: INTRODUCTION

### **Alzheimer's Disease**

Alzheimer's disease (AD) is a neurodegenerative disease encompassing the most prevalent form of dementia characterized by beta-amyloid plaques ( $\beta$ AP) and neurofibrillary tangles (NFTs) (DeTure & Dickson, 2019; Martins et al., 2006). Early-onset AD has been associated with autosomal-dominant mutations in the amyloid precursor gene (*APP*), presenilin-1 and -2 (*PSEN1/PSEN2*) genes (Martins et al., 2006). These mutations collectively comprising what is known as early-onset AD, affect approximately 5% of all known AD cases (Association, 2019). The majority of AD cases are characterized as late-onset in which the highest risk factors for the disease are environmental (e.g., aging and lifestyle choices) in addition to the inheritance of an apolipoprotein (*APOE*) allele, namely apolipoprotein E4 (*APOE4*) (Martins et al., 2006). The *APOE* gene has several isoforms of importance that are affected by a cysteine to arginine polymorphism: *APOE2* (C<sup>112</sup>, C<sup>158</sup>), *APOE3* (C<sup>112</sup>, R<sup>158</sup>), and *APOE4* (R<sup>112</sup>, R<sup>158</sup>) (Munoz et al., 2018; Weisgraber, 1994). A carrier of the *APOE4* allele increases the risk of developing AD by four to twelve-fold (Martins et al., 2006). However, the mechanisms of how ApoE4 contributes to increased risk of disease have remained elusive.

### **ApoE4 Structure and Function**

The *APOE* gene encodes the main cholesterol transporter protein (ApoE) in the CNS that is associated with use of low-density lipoprotein receptor (LDLR) family

(Goldstein & Brown, 1976; Innerarity & Mahley, 1978). Cholesterol transport in both the periphery and the CNS are vital for basal cellular function, but neurons are in critical need of adequate supply for synaptogenesis and neurite outgrowth (Xie et al., 2003). Full length ApoE isoforms are 299 amino acids (AA) long with a molecular weight (MW) of 34 kDa. ApoE has 2 major domains: a lipoprotein receptor binding N-terminal, a lipid and A $\beta$  binding C-terminal that connect via a hinge region (Mahley, 2016). The ApoE isoforms differ in receptor binding affinity through the stepwise change in cysteine (C) to arginine (R) from ApoE2 to ApoE4 (Weisgraber, 1994). The C<sup>112</sup> to R<sup>112</sup> mutation alters the side chain orientation of ApoE4 compared to ApoE2 and ApoE3 through the formation of a salt bridge combining R<sup>112</sup> to E<sup>109</sup> (Buttini et al., 1999; Weisgraber, 1994; Xie et al., 2003). Changes in the conformational structure of the isoforms from the C to R substitutions leads to an increased likelihood of the proteolysis for ApoE4> ApoE3>ApoE2 by exposing previously confined proteolytic cleavage sites in the hinge region (Harris et al., 2003). The role of ApoE4 proteolysis as an early pathophysiological event for AD development has been supported through the findings of fragments that hold neurotoxic effects on the CNS with varying degrees of severity that appear dependent on size and location of the fragmentation of ApoE (Dafnis et al., 2012; Zhou et al., 2006). Size and location of the fragmentation events is dependent on the cleavage enzymes utilized. Our lab formerly presented data on an ApoE4 fragment identified in the prefrontal cortex from post-mortem AD patient tissue and that localize within NFTs (Rohn et al., 2012). Our findings demonstrated that exogenous application of a smaller amino-terminal fragment of ApoE4 (nApoE4<sub>1-151</sub>) that is 1-151 amino acids in length to microglial cells resulted in uptake of nApoE4<sub>1-151</sub>, trafficking to microglial nuclei, and the



upregulated expression of genes associated with inflammation (Cho et al., 2001; Love et al., 2017) Our previous findings also supported a role for the matrix metalloproteinase-9 (MMP-9) in generating this fragment due to its' ability to cleave ApoE4 at D<sup>154</sup> generating a 17 kDa fragment as observed previously within AD post-mortem brain tissue (Love et al., 2017). MMP-9 and ApoE have both previously been linked to the activation of inflammatory pathways within the context of AD (Cho et al., 2001). However, increased prevalence of proteolysis for ApoE4 is only a piece to this puzzle. The fragmentation of ApoE4 into a 17 kDa fragment via MMP-9 occurs in the extracellular matrix. Studies investigating the downstream effects of fragmentation have demonstrated localization of fragments in cell nuclei, where ApoE4 fragments have the potential to act as transcription factors to upregulate inflammatory responses in microglia and neurons (Dafnis et al., 2012; Gottschall & Deb, 1996). The missing link between these steps is the process of re-internalizing the ApoE fragment once it has been cleaved. Interaction with low-density lipoprotein receptor related protein (LRP) and a thrombin-cleaved 22 kDa N-terminus ApoE4 fragment showcase a plausible uptake mechanism via receptor mediated endocytosis (Tolar et al., 1997). This uptake by the LRP is typically observed with lipoprotein bound ApoE but is seen to occur with un-enriched ApoE in the case of fragmentation where the LDL binding region is intact (Narita et al., 2002; Wilson et al., 1991). Once the smaller fragment can re-enter the intracellular environment, ApoE4 fragments are able to diffuse through the nuclear pore to act as potential regulators of gene expression. The process detailed above describes a model in which ApoE4 has the propensity to play a direct role in the pathophysiological progression of AD through actions as a transcription factor in upregulating pro-inflammatory responses.

The results previously described by our lab were generated using a transformed BV2 microglial cell line, *in vitro*, to understand the potential effects of the fragment in the cellular environment; this data has been expanded within my thesis to provide biological context to the results through an *in vivo* study on the organismal effects of ApoE4 fragmentation by utilizing a vertebrate animal model: zebrafish (*Danio rerio*).

### **Zebrafish as a Model for Alzheimer's Disease**

The zebrafish model system has increasingly been used to study neurobiological questions in vertebrates. Some of the many benefits to this model are the rapid growth cycle, high fecundity rates, transparency of embryogenesis via externally fertilized embryos, and the early generation of stereotyped behavior during embryonic and larval stages (Gottschall & Deb, 1996; Narita et al., 2002; Tolar et al., 1997). Documentation of the zebrafish embryogenesis process has been well-documented for organ, tissue, cell, and molecular contexts. The zebrafish has a duplicated genome with split or lost function among the duplicated genes (Horzmann & Freeman, 2018). The zebrafish, while not as complex as a rodent model, shares many developmental conserved neurochemical and neuroanatomical pathways with humans (Beckers et al., 2019; Nesan & Vijayan, 2012). While not all structures in human brains are directly transferrable in structure to the zebrafish brain, comparable cellular networks exist which follow similar developmental progression to humans (Kimmel et al., 1995; Schmidt et al., 2013). An applicable example for our research is the lack of a formalized hippocampus region in zebrafish. The hippocampus is recognized as the primary location for memory integration and retention in the human brain which takes on heavy burden with A $\beta$  and NFT accumulation in AD (He et al., 2018). Zebrafish lack a defined structure to date for a

zebrafish hippocampus, a comparative neuronal population in the pallium has been shown to function as an effective homologue to the hippocampus in mammals which then provides a function comparison (Portavella et al., 2004; Vargas et al., 2012). In addition to structural similarity, zebrafish contain orthologs for genes associated with the progression of AD in humans such as those demonstrated in **Table 1**. Ortholog presence can provide realistic expectations for the biological mechanisms that take place for AD-associated abnormalities such as the presence of *mapta* and *maptb* in zebrafish. The *mapt* orthologues in zebrafish correspond to the human *MAPT* which encodes for a protein highly correlated with neurodegenerative disease: Tau. Tau is a microtubule associated protein (MAP) which is hyperphosphorylated in AD leading to aggregation into what are known as tau tangles (DeTure & Dickson, 2019). The endogenous presence of tau via *mapta* and *maptb* create ample model to study the development of tauopathies. The combined attributes of the zebrafish model system make it an ideal vertebrate species to add biological relevance to AD research.

### **Hypothesis**

My thesis using zebrafish represented a logical progression of previous work in the lab following the *in vitro* BV2 cell culture studies (Love et al., 2017; Pollock et al., 2020; Pollock et al., 2019). Other studies have demonstrated the neurotoxic effects of fragmentation in ApoE4 as well as neuroprotective effects of ApoE3 fragmentation (Buttini et al., 1999; Tolar et al., 1997). Based on prior data completed *in vitro*, data supporting the role in a vertebrate system is necessary to understand the role of ApoE fragmentation in a complex tissue environment. The overarching hypothesis of my thesis is that treatment of zebrafish embryos with nApoE4<sub>1-151</sub> will lead to morphological,

behavioral, and molecular abnormalities supporting the role of ApoE4 fragmentation as a crucial step in AD pathogenesis.

## Tables

**Table 1. Overview of AD associated genes in human versus zebrafish.**

Gene sequence analyses can be compared to understand similarities between human and protein similarity.

Name	Zebrafish Gene(s)	Function(s)	Location(s)	Sequence Homology	References
APOE	<i>apoec</i>	Cholesterol Transport	Retina, YSL, CNS	27.5%	(Babin et al., 2014)
	<i>apoeb</i>			25.6%	
APP	<i>appa</i>	Axonal outgrowth, synaptogenesis	CNS	70.0%	(Musa et al., 2001)
	<i>appb</i>			67.0%	
MAPT	<i>mapta</i>	microtubule binding	CNS, <i>maptb</i> only in spinal cord	43.8%	(Howe et al., 2020)
	<i>maptb</i>			57.0%	

## CHAPTER TWO: MORPHOLOGICAL EFFECTS

### Overview

As an initial approach, we examined the developmental effects of exogenous treatment of hatching stage zebrafish embryos following treatment with nApoE4<sub>1-151</sub> at the beginning of the segmentation period. The timepoint of 24 hours were chosen as a starting point for treatment because after 24 hours post-fertilization (hpf), embryo survivability in untreated control AB-wild-type (ABWT) embryos were 100%. From 0 hpf to 24 hpf, embryos had approximately 75-80% survival which can confound data on survivability within that time frame. Due to the steep curve in survivability prior to 24 hpf, treatment was initiated between the somite-19 and prim-5 stages (Kimmel et al., 1995). A set staging range during the treatment of zebrafish was applied by gauging the stages of development through Kimmel et al. (1995) standards (**Table 2**). For zebrafish, embryogenesis is asynchronous both across and within clutches which can lead to misrepresentation of development progress across embryos without an applied set standardization (Kimmel et al., 1995). Primarily, for treatment, head to tail positioning, and the counting of somite under a microscope were employed to determine the staging period of each embryo selected as shown. The selection process during treatment was vital in allowing analysis of developmental features in a constructive format that allowed results on development to be compared across groups in this project. This chapter employed a semi-qualitative scale, heart rate measurements, and survivability to inform observations about zebrafish development across treatment groups for non-treated

zebrafish (control), nApoE3<sub>1-151</sub>, and nApoE4<sub>1-151</sub> treated samples. My working hypothesis is that nApoE4<sub>1-151</sub> will show developmental progress that is disrupted when compared to untreated controls or to nApoE3<sub>1-151</sub> treated samples.

## **Materials and Methods**

### Synthesis of nApoE<sub>1-151</sub> fragments

Generation of nApoE4<sub>1-151</sub> and nApoE3<sub>1-151</sub> including synthesis of plasmids, expression in *E. coli*, and purification (>85% purity) was contracted out to GenScript Inc. (Piscataway, NJ). A 6X His-tag at the C-terminal end was added to facilitate purification. The protein fragments are identical aside from the C<sup>112</sup> to R<sup>112</sup> replacement in nApoE4<sub>1-151</sub>. The verification of proteins was rigorous with each preparation including a certificate of analysis that includes DNA sequencing, SDS PAGE, and western blot by using standard protocols for molecular weight and purity measurements. The concentration of recombinant proteins was determined by Bradford protein assay with BSA as a standard. Characterization of nApoE4<sub>1-151</sub> in our laboratory was assessed by ELISA and western blot analysis utilizing an anti-His antibody as previously described in (Pollock et al., 2019). A similar fragment to apoE3 (nApoE3<sub>1-151</sub>) was utilized to directly compare the differences in toxicity and nuclear localization between nApoE4<sub>1-151</sub> and nApoE3<sub>1-151</sub>.

### Zebrafish Embryo Care and Maintenance

Animal husbandry and colony maintenance was handled by the Boise State University vivarium system. All animal protocols are coordinated with the Boise State University IACUC committee in accordance with recommendations from the Zebrafish Information Network (Zfin), IACUC protocols #AC18-011 and #AC21-009. Embryos

were reared at 28.5°C in an enclosed incubation unit until treatment with exogenous protein fragment.

#### Treatment of Embryos with exogenous ApoE<sub>1-151</sub> fragments

Treatment of embryos began at 24 hpf during the 19-somite-prim-6 stage in accordance with the Kimmel Staging Series (Kimmel et al., 1995). Zebrafish embryos that were staged at the time of treatment to be above 24 hours (prim-5) or below 19 hpf (20-somite stage) were excluded from experimentation. Incubation of embryos was accomplished using a mixture of E3 media with various concentrations of nApoE<sub>4<sub>1-151</sub></sub> or nApoE<sub>3<sub>1-151</sub></sub> protein fragments. Following staging assessments, embryos were allocated to an incubation chamber in an even distribution depending on experiment. Embryos were kept with a density of no more than 5 embryos in a minimum of 100 µL of E3 media + protein fragment per well for a 96 well plate. Control groups were raised in identical conditions with the only difference being the absence of nApoE<sub>1-151</sub> fragments present in E3 media. Embryos were then placed in incubator for 24 hours of undisturbed incubation at 28.5°C before being collected for experimentation.

#### Live Imaging (Light Microscope)

Live observations were recorded on an EVOS M5000 Light Microscope using brightfield settings. Embryos were imaged at 4X for a general view of the embryo(s) and 10X or greater were used for tissue specific image acquisition. Mortality was assessed as described below by comparing the number of nominal labels (1=Alive, 0= Dead/Non-viable) given to each group. A tally was taken via a contingency table in R to provide a raw count for each individual treatment group. Normality and equal variance were tested for prior to analysis. Each group count was then tested against each other via a Chi-



square analysis and displayed via a mosaic display to indicate statistical significance by shading and examination of the Pearson residual values.

### Morphological Assessments

A set scale was generated across multiple standards resulting in a developmental abnormality score (**Figure 1**). Embryos were scanned throughout the z-axis to identify pigmentation, and gauge organogenesis at specific stages in coordination with the Kimmel staging series. Results were then compared to untreated controls and the comparable nApoE3<sub>1-151</sub> treatment groups.

### Heart Rate Determination

Live imaging was also applied for mortality assessments of embryos in the manner of identifying heartrate over the course of 10 second intervals. If no heart rate was detected, stimulation of embryo through water movement was performed to verify lack of response to stimuli. If no response to stimulation was found in combination with a lack of heartbeat, subject was deemed non-viable. Heart rate was measured in a continuous manner by beats per minute (bpm) as described above. Samples were averaged by replicate to stabilize variation within groups. Five sets of heart rate collection dates were tested through two-way ANOVA modelling with three treatment groups (Control, nApoE3<sub>1-151</sub>, and nApoE4<sub>1-151</sub>) in R statistical software. ANOVA model was assessed for assumptions after creation of model in R.

## **Results**

### Embryonic Survivability

Survivability of embryos beginning with fragment treatment at 24 hpf resulted in a 90-100% reduction in viable embryos 48 hours after treatment began. nApoE4<sub>1-151</sub>

treated samples failed to recover after removal of treatment media. The survivability of nApoE4<sub>1-151</sub> at a concentration of 25 µg/ml was reduced by 50% within 24 hours of treatment, whereas nApoE4<sub>1-151</sub> at 50 µg/mL reduced survivability by 50% in under 12 hours. In contrast, similar concentrations of nApoE3<sub>1-151</sub> resulted in a smaller decline in survivability (<15%).

### Developmental Abnormalities

Developmental abnormalities produced higher scores within nApoE4<sub>1-151</sub> treated samples compared with controls at the highest concentration level for 48 hpf ( $H(4)=-3.32$ ,  $p=0.0004$ ). nApoE3<sub>1-151</sub> also showed an increase in scores that appears treatment level dependent (see **Figure 3D**) but lacked statistical significance from nApoE4<sub>1-151</sub> groups. The highest treatment level for nApoE3<sub>1-151</sub> was significantly different from controls ( $H(4)=-1.77$ ,  $p=0.037$ ). Features most commonly observed for nApoE4<sub>1-151</sub> groups were lack/less pigmentation, lack of hindbrain folding at cerebellar primordium, lack of detectable heartbeat/no response to stimulus, etc. Features most commonly observed in nApoE3<sub>1-151</sub> treated samples were less pigmentation and deformed yolk sac. Each group began to have a distinct appearance following treatment as shown in **Figure 3A-C**.

### Heart Rate

Heart rate in the highest (50 µg/mL) nApoE4<sub>1-151</sub> treatment group decreased by 50% compared with controls and nApoE3<sub>1-151</sub> treated samples. The lowest nApoE3<sub>1-151</sub> treated samples were different from the highest treatment of nApoE4<sub>1-151</sub> but not from controls.

## Conclusions

Assessing morphological changes following treatment with an amino-terminal fragment of ApoE4 is a valuable application of *in vivo* research to understand the biological context with which the molecular events. As shown in this chapter, treatment with nApoE4<sub>1-151</sub> has concentration-dependent impact on decreasing survivability, decreasing heart rate, as well as adversely affecting developmental embryogenesis. Treatment with nApoE3<sub>1-151</sub> fragment in an identical fashion does not appear to hinder development of embryos. Survivability curves indicate the effects from ApoE4 treatment are long lasting and no recovery was observed in nApoE4<sub>1-151</sub> survivability rate from 48-72 hpf after the treatment period had ended. Developmental abnormalities were observed following treatment with nApoE4<sub>1-151</sub>. Abnormalities frequently reported using well-defined criteria (**see Figure 1**) included: enlarged heart, enlarged pericardial cavity, limited pigmentation, and limited hindbrain folding. Results indicate disruption to normal development throughout the nervous and cardiovascular system following treatment with nApoE4<sub>1-151</sub>. Some of the effects that were noted in nApoE4<sub>1-151</sub> were also present in the nApoE3<sub>1-151</sub> which were expected to behave more akin to the untreated control group; this will be explored in the discussion chapter. However, the results for nApoE4<sub>1-151</sub> highlight an important role for the ApoE4 fragment in causing toxicity and support our previous *in vitro* findings (Love et al., 2017; Pollock et al., 2020).

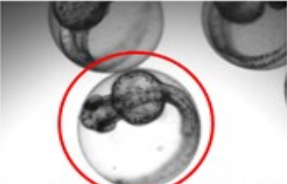

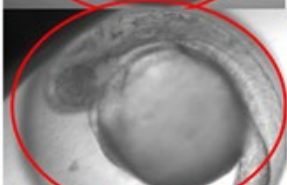

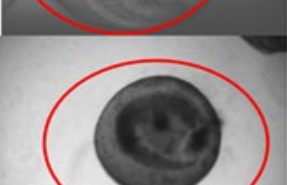
## Tables

**Table 2 Stages of Embryonic Development (Condensed from (Kimmel et al., 1995)). Stages of development were assessed by evaluating the embryos in our projects in comparison to the scale provided below. Morphological features provided in the table were then used to set a normal developmental timeline criteria for controls.**

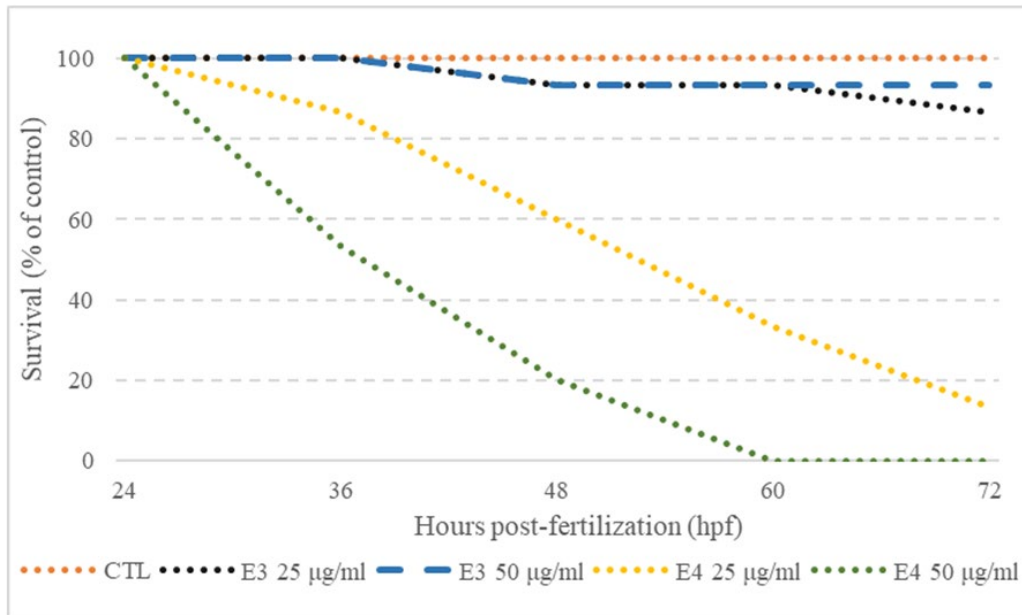
Stage	HPF	Features
<b>Zygote</b>		
1-cell	0	Cytoplasm streams toward animal pole to form blastodisc
<b>Segmentation period</b>		
1-somite	10 1/3	First somite furrow
5-somite	11 2/3	Polster prominent, optic vesicle, Kupffer's vesicle
14-somite	16	Otic placode, brain neuromeres, v-shaped trunk somites, Yolk Extension visible
20-somite	19	Muscular twitches, lens, otic vesicle, rhombic flexure, hindbrain neuromeres prominent, tail can extend
26-somite	22	side-to-side flexures, otoliths, Prim-3
<b>Pharyngula Period</b>		
Prim-5	24	HTA= 120°, OVL=5, YE/YB=1, early pigmentation in retina and skin; median fin fold, red blood cells on yolk, heartbeat detectable
Prim-15	30	EL=2.5mm, HTA=95°, OVL= 3, YE/YB>1, YB/HD=2, early touch reflex and spontaneous movements, retina pigmented, dorsal stripe to somite 12, weak circulation
Prim-25	36	EL=2.9mm, HTA=75°, OVL=3, PF(H/W)= 3/4; early motility, tail pigmentation, ventral stripe, strong circulation, single aortic arch pair, pericardium not swollen
High-pec	42	EL=2.9mm; HTA=55°, OVL<1 and >1/2, YE/YB=1.5, YB/HD <1.3 PF(H/W)=1; dechlorinated embryos rest on side, YE cylindrical, PF apical ridge prominent, early larval stripe, xanthophores in head only, iridophores in retina only, pericardium prominent
<b>Hatching Period</b>		
Long-pec	48	EL=3.1 mm, HTA=45°, OVL=1/2, PF(H/W)= 2, resting dorsal up, YE beginning to tape, PF pointed, dorsal and ventral stripes meet at tail, ca. 6 melanophores in lateral strip, iridophores fill retina, yellow cast to head
Pec-fin	60	EL=3.3mm; HTA=35°, YB tapering into YE, upto 10 melanophores in vertical stripe, PF flattened into fin shape with prominent circulation, early jaw cartilage, circulation in 5-6 AA, mouth remains small and open at ventral location midway between eyes
Protruding Mouth	72	EL=3.5mm; HTA=25°, wide open mouth protruding anterior to eye, iridophores in yolk stripe, eye half covered by iridophores, dorsal body as yellow as head

## Figures

**Scale for Developmental Abnormalities**

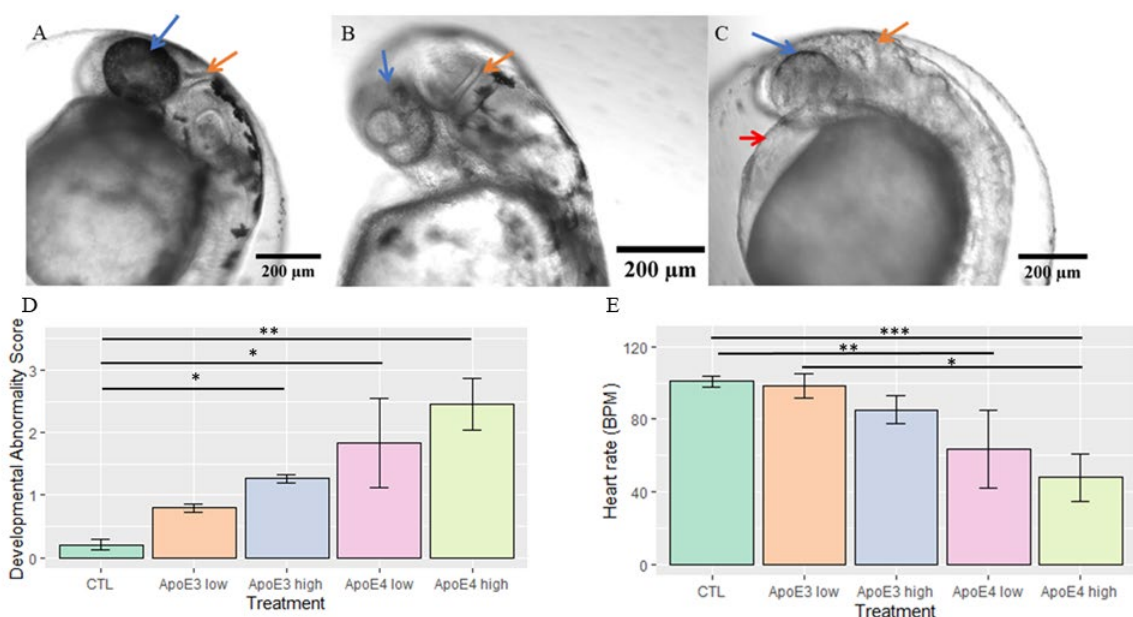
Descriptor	Characteristics	Score	Visual Comparison
No noticeable abnormalities	Appear to match developmental markers: Embryo is clean No abnormality can be visually identified Proper pigmentation displayed Appears to be estimated developmental stage	0	
Minimal Abnormality	Does not meet 1 developmental standard: No observable hindbrain folding Delay or lack of ear development deformed/misshapen yolk sac Enlarged cardiac cavity Normal Pigmentation	1	
Some Abnormalities	Does not meet 2 developmental standards: No observable hindbrain folding Delay or lack of ear development Deformed/misshapen yolk sac Enlarged cardiac cavity Craniofacial abnormality	2	
Moderate Abnormalities	Does not meet 3 developmental standards: No observable hindbrain folding Delay or lack of ear development Deformed/misshapen yolk sac Enlarged cardiac cavity Craniofacial abnormality	3	
Extreme Abnormality	Meets any of the following standards: No heart rate No discernible shape Blackened or cloudy	4	

**Figure 1. Project specific developmental abnormality scale.**  
Project scale was determined as a semi-qualitative measure for observing changes across treatment groups. Scale was generated following observation of 30 embryos per treatment group.



**Figure 2. Survivability decreased in zebrafish embryos following exogenous treatment with an amino-terminal fragment of nApoE4<sub>1-151</sub>.**

Embryos at 24hpf (prim-9 stage) were segregated into three groups: controls (untreated), 25 µg/mL or 50 µg/mL nApoE3<sub>1-151</sub>, and 25 µg/mL or 50 µg/mL nApoE4<sub>1-151</sub>. Embryos that lacked a heartbeat for 10 seconds were stimulated to induce movement. If no movement or heartbeat was detected, embryos were considered to be non-viable. Data represent 3 independent trials, n=5 fish/treatment.



**Figure 3. A sublethal concentration of nApoE4<sub>1-151</sub> leads to morphological abnormalities in zebrafish embryos at the hatching phase.**

Representative light phase contrast microscopic images following live imaging of embryos at 48hpf following a 24-hour period with respective treatments (Control, 25  $\mu\text{g}/\text{mL}$  of nApoE3<sub>1-151</sub>, or 25  $\mu\text{g}/\text{mL}$  of nApoE4<sub>1-151</sub>). A: Arrows point to consistent morphological changes as compared to untreated controls that are healthy and categorized as having a developmental abnormality score of  $<1.0$  (Panel A). The blue arrows designate pigmentation changes; orange arrows designate cerebellar primordium junction differences in the hindbrain. B: Exogenous treatment with nApoE3<sub>1-151</sub> impacted pigmentation pattern in otherwise healthy embryos. Embryos in this category were most likely to receive a score of  $<1$ . C: 24-hour incubation of a sublethal concentration of nApoE4<sub>1-151</sub> resulted in developmental abnormality scores  $>3$ . Embryos in this category were typically observed to be delayed in development with limited hindbrain folding (orange arrow), limited or lacking pigmentation (blue arrow), as well as enlargement of the cardiac cavity (red arrow). D. Quantitative developmental abnormality scores for each treatment group following treatment of embryos for 24 hours with respective E3 (orange bar), E4 (gray bar) at 25  $\mu\text{g}/\text{mL}$  and E3 (gray bar), E4 (yellow bar) at 50  $\mu\text{g}/\text{mL}$ .

nApoE4<sub>1-151</sub> 25  $\mu\text{g}/\text{mL}$  was significantly different from controls ( $H(4)=-2.43$ ,  $p=0.0074$ ). nApoE4<sub>1-151</sub> 50  $\mu\text{g}/\text{mL}$  was significantly different from controls ( $H(4)=-3.32$ ,  $p=0.0004$ ).

nApoE3<sub>1-151</sub> was different from controls ( $H(4)=-1.77$ ,  $p=0.037$ ) All other comparisons were not significant. Errors bars represent  $\pm$ S.E.M., Control( $n=5$ ), E325 and E350( $n=2$ ), E425 and E450 ( $n=4$ ). \* $p<0.05$ , \*\* $p<0.01$ , \*\*\* $p<0.001$  E. Heart rate data obtained from live microscope analyses in 25  $\mu\text{g}/\text{mL}$  and 50  $\mu\text{g}/\text{mL}$  treatment groups nApoE3<sub>1-151</sub> and nApoE4<sub>1-151</sub> compared to non-treated controls. nApoE4<sub>1-151</sub> 25  $\mu\text{g}/\text{mL}$  was significantly different from controls ( $H(4)=1.77$ ,  $p=0.038$ ). nApoE4<sub>1-151</sub> 50  $\mu\text{g}/\text{mL}$  was significantly different from nApoE3<sub>1-151</sub> 25  $\mu\text{g}/\text{mL}$  ( $H(4)=1.94$ ,  $p=0.026$ ) and controls ( $H(4)=2.665$ ,  $p=0.0039$ ). Errors bars represent  $\pm$ S.E.M., Control( $n=5$ ), E325 and E350( $n=2$ ), E425 and E450 ( $n=4$ ). All other comparisons were insignificant. \* $p<0.05$ , \*\* $p<0.01$ , \*\*\* $p<0.001$

### CHAPTER THREE: MOLECULAR EFFECTS

In the present chapter, the effects of nApoE<sub>4</sub><sub>1-151</sub> were examined from a molecular context. The proposed experiments provide proof of concept for the *in vitro* research performed previously by our lab with the nApoE<sub>1-151</sub> fragments and BV2 microglial cells. In this chapter, a lactate dehydrogenase (LDH) assay was undertaken using zebrafish homogenates to assess cytotoxicity. The LDH assay reports levels of cytotoxicity by quantifying the release of LDH through a chain reaction that precipitates a color change proportional the amount of LDH that is in the medium (Scientific). This assay typically works with specificity since LDH is a cytosolic enzyme found within cells. When a cell incurs damage to the plasma membrane, this allows for the cytosolic enzyme to enter the prepared media (Lungu-Mitea et al., 2021). Our study adjusted the use guidelines proposed in (Diamantino et al., 2001; Maharajan et al., 2018) to raise the number of 48 hpf embryos to 15 per sample group. Identification of a known apoptotic marker, activated, cleaved caspase-3 (17 kDa and 19 kDa), was also employed to assess the activation of apoptotic pathways as a mechanism of cell death (Lossi et al., 2018).

Previous studies performed in our lab were restricted by utilizing transformed, BV2 microglial cell lines (Love et al., 2017). By using a single cell type, the research lacks information on whether nApoE<sub>4</sub><sub>1-151</sub> interacts with neurons and more specifically could also traffic to the nucleus similar to the results from BV2 microglial cells. Trafficking to the nucleus is a vital step in understanding whether the actions of nApoE<sub>4</sub><sub>1-151</sub> are direct through a role as a transcription factor or through an indirect mechanism. The extension of our previous work into a complex tissue environment fills a



gap in the knowledge of how nApoE4<sub>1-151</sub> might interact with various cell types including neurons. Immunohistochemical methods such as immunofluorescence were applied to look examine cellular localization of ApoE fragments compared to untreated controls. To accomplish this goal, the ApoE fragments were synthesized with 6X-His-tag which allows for the identification of the fragments in culture or tissue experiments through the application of an anti-6X His-tag antibody. To identify neuronal cells, a NeuN antibody was applied to zebrafish sections. The NeuN reacts to *rbfox3*, a neuron specific nuclear protein. Additionally, utilizing an organismal system with orthologues similar to those expressed in AD (*MAPT*; *mapta* and *maptb*) allowed the opportunity to screen for AD-like tau pathology using triple label confocal microscopy. Immunostaining was performed on fixed zebrafish tissue sections utilizing PHF-1, a marker for hyperphosphorylated Tau at S396/404. My working hypothesis for this the first half of this chapter is that we will detect increased cytotoxic biomarkers in nApoE4<sub>1-151</sub> over control and nApoE3<sub>1-151</sub> treatment groups. For the second half of the chapter, we predict that nApoE4<sub>1-151</sub> will be detected within neuronal nuclei and develop potential tau pathology compared to control or nApoE3<sub>1-151</sub> treated groups.

## **Materials and Methods**

### Zebrafish Homogenate Preparation and Cytotoxic Assays

Samples for analysis in Pierce Lactate Dehydrogenase (LDH) and western blot were generated by homogenizing 15 embryos per treatment over ice in 0.1 M Tris-HCL, pH,7.2. Homogenized samples were then centrifuged at 3000 x g for 5 minutes at 4°C. The supernatant was then collected for use in LDH and western blot analysis. LDH measurements and western blot analyses were conducted as previously described utilizing

whole embryo homogenates (Love et al., 2017). Briefly, to determine the involvement of caspase-3, we utilized the cleaved caspase-3 (1:1,000) antibody from Cell Signaling Technology, which detects both the 17 and 19 kDa active domains of caspase-3. To ensure equal protein loading among various samples, embryo homogenates were assayed (BCA) for protein content. In addition, transferred SDS-PAGE gels were stained with Coomassie blue to ensure equal protein loading.

### Immunohistochemistry

For all immunohistochemical procedures in this study, a standard protocol was followed for tissue preparation, and preparation of the slides. At the conclusion of treatment experiments, embryos were sacrificed prior to manual removal of chorion. Following de-chorionation, embryos were fixed in 4% paraformaldehyde (PFA)/PBS overnight at 4°C and prepared for 5 µm paraffin-embedded sectioning using a Leica RM2235 Microtome at 4 °C. After slide preparation. Paraffin-embedded sections were used for staining following rehydration and a series of washes in phosphate-buffered saline with 0.05% Tween 20 (PBT). Blocking of sections for non-specific staining was accomplished using a standard incubation buffer consisting of 1% Normal Goat Serum, 2% Bovine Serum Albumin in PBT for 2 hours at room temperature (RT). Primary antibodies, detailed in **Table 3**, were incubated with slides for 18-24 hours at 4°C. Sections were then washed in triplicate for 5 minutes with PBT. Slides were then incubated in the appropriate secondary antibody for 1 hour at RT. Following the final wash, DAPI (nuclear stain) -infused soft mount was placed on slides and allowed to set before coverslip addition. Sections were assessed for preliminary staining with EVOS M5000 light cubes at lowest intensity settings. Sections were then kept in the dark at 4°C

until used for confocal imaging. Confocal assessment of the localization of nApoE4<sub>1-151</sub> in neuronal cell populations was as previously described. All images and z-stacks generated were obtained using Zeiss Microscope, LSM 510 Meta confocal imaging system (Carl Zeiss, Oberkochen, Germany) and processed using Zen blue edition (Carl Zeiss, Göttingen, Germany).

## Results

### Toxicity

Using methods detailed in chapter one, 48hpf nApoE4<sub>1-151</sub> treated samples contained more than expected non-viable embryos classified by our standards of lacking a heartbeat and being unresponsive to stimulation ( $p=1.17 \times 10^{-13}$ ) (**Figure 4A**).

### Pierce Lactate Dehydrogenase Assay

Treatment of zebrafish embryos with exogenous nApoE4<sub>1-151</sub> led to an increase in the release of LDH, however, no significance was determined (**Figure 4B**). LDH release is a down-stream indicator of cell death or damage to the plasma membrane. Control groups represent the baseline expectation for comparison.

### Caspase-3 Western Blot

Activated caspase-3 was identified in nApoE4<sub>1-151</sub> treated samples using an antibody that recognizes cleaved caspase-3 peptides (17 and 19 kDa), but not in untreated controls. Coomassie blue staining of transferred gel slabs indicated an equal protein loading in both untreated controls and nApoE4<sub>1-151</sub> treated sample groups (see **Figure 4C**). Equal protein loading with detection of cleaved caspase-3 indicates activation apoptotic pathways following treatment of zebrafish embryos with 50 µg/mL nApoE4<sub>1-</sub>

### Immunohistochemistry

Triple label confocal microscopy confirmed nuclear staining in nApoE4<sub>1-151</sub> treated samples, where peri-nuclear staining was observed in nApoE3<sub>1-151</sub> in NeuN labeled neurons (see **Figure 5**). In parallel experiments, we examined whether we could detect tau pathology using the PHF-1 antibody. As depicted in Figure 7, labeling of PHF-1 in nApoE4<sub>1-151</sub> treated samples was present and more distinguishable than in controls or nApoE3<sub>1-151</sub> treated samples for 48 hpf (see **Figure 6**) and more distinguishable than controls at 72 hpf (see **Figure 7**).

### **Conclusions**

LDH results demonstrated that following exogenous treatment with nApoE4<sub>1-151</sub> increased cytotoxicity in a concentration-dependent manner. Activated caspase-3 detection supports a role for the activation of apoptotic pathways as a mechanism of cell death. Results from confocal experiments supports the hypothesis that nApoE4<sub>1-151</sub> traffics to neuronal cell nuclei. Finally, results from triple-label confocal microscopy support the presence of tau pathology in nApoE4<sub>1-151</sub> treated samples as compared to the controls or the nApoE3<sub>1-151</sub> group in 48 hpf samples. Data looking at 72 hpf was more compelling, identifying that at 24 hpf post treatment, tangle pathology is present and not observed in non-treated controls.

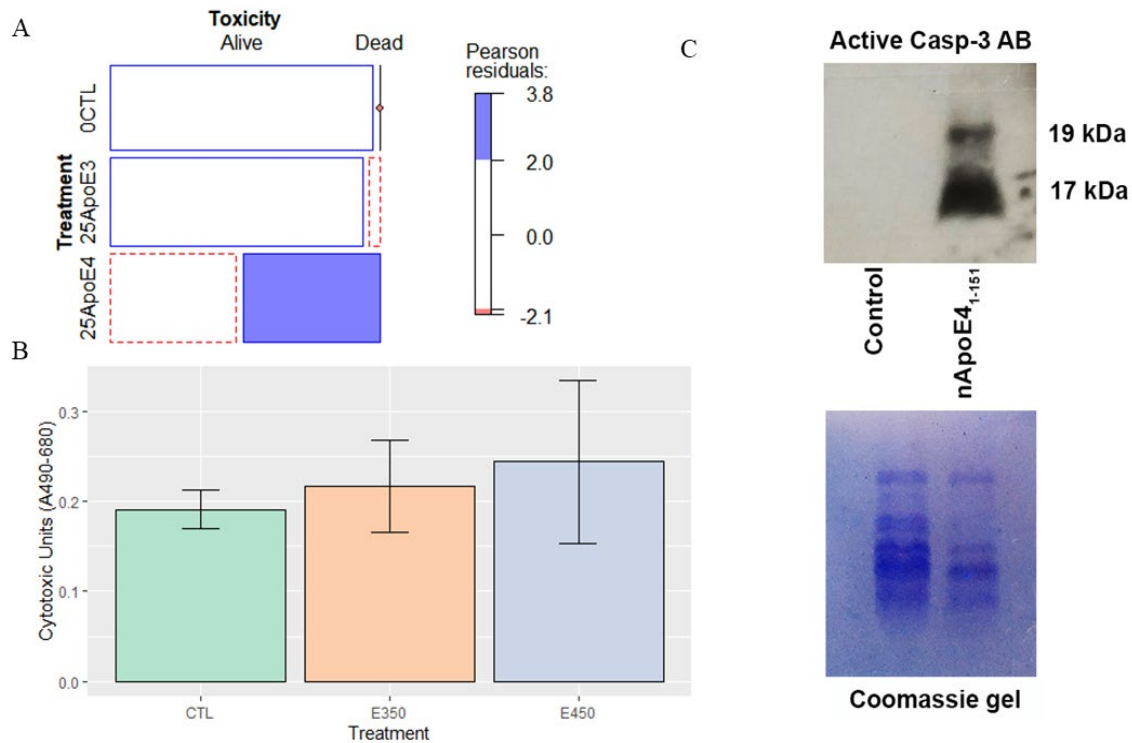
## Tables

**Table 3. Antibodies used in Immunohistochemistry Experiments.**

Antibodies were used in immunohistochemistry experiments detailed above. Anti-6x His Tag antibodies were used to identify recombinant ApoE fragments in conjunction with either NeuN or PHF-1 for experiments.

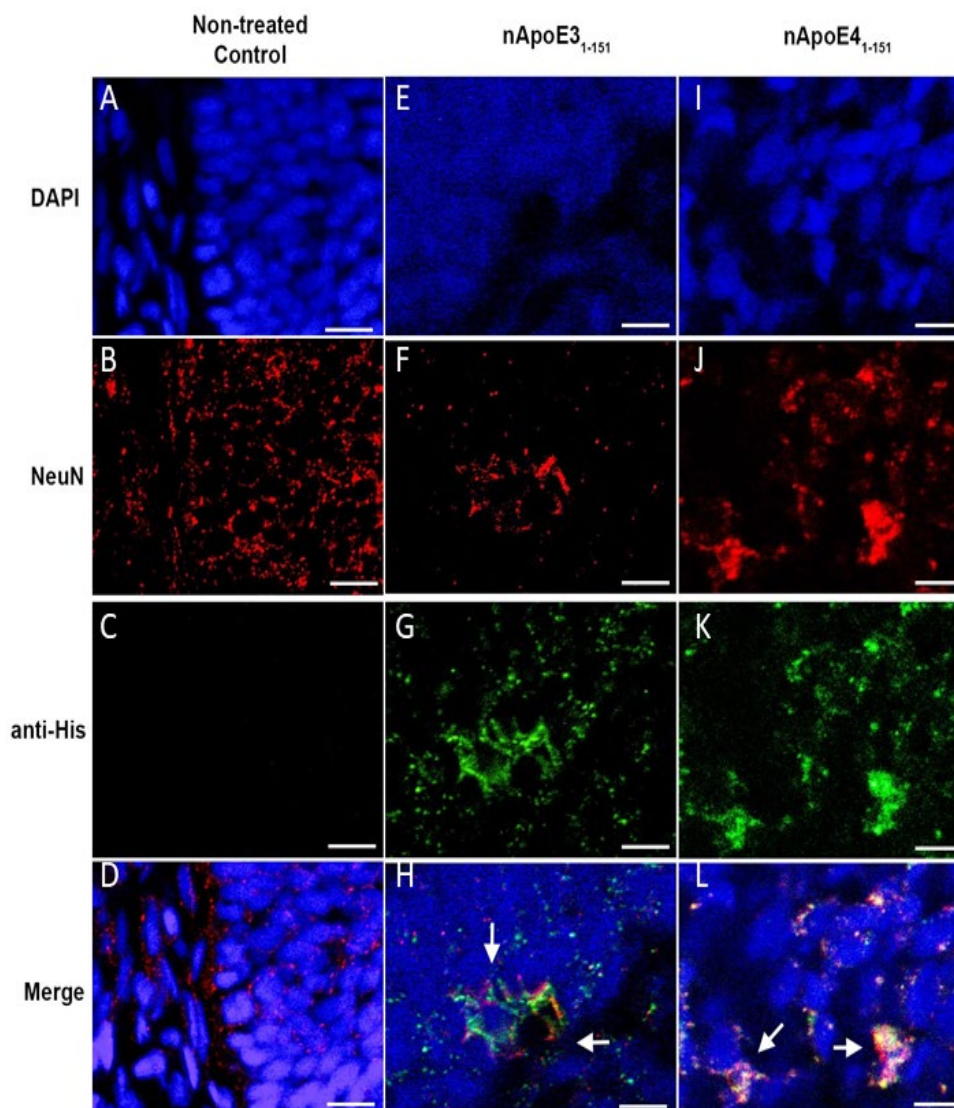
Primary Antibodies	Reactivity	Secondary Antibodies	Source
Anti-6x His Tag (1:500, Rabbit polyclonal)	nApoE3 <sub>1-151</sub> and nApoE4 <sub>1-151</sub>	AF 488 (1:500, Goat, Anti-Rabbit)	Abcam, Inc, ThermoFisher
NeuN (1:50, Mouse polyclonal)	rbfox3a, Neuronal nuclei	AF 555 (1:200, Donkey, Anti-Mouse)	Abcam Inc, ThermoFisher
PHF-1 (1:250, Mouse polyclonal)	Tau phosphorylated 396 and 404	AF 555 1:200, Donkey, Anti-Mouse)	Dr. Pete Davies (Albert Einstein College of Medicine, Bronx, NY), ThermoFisher

## Figures



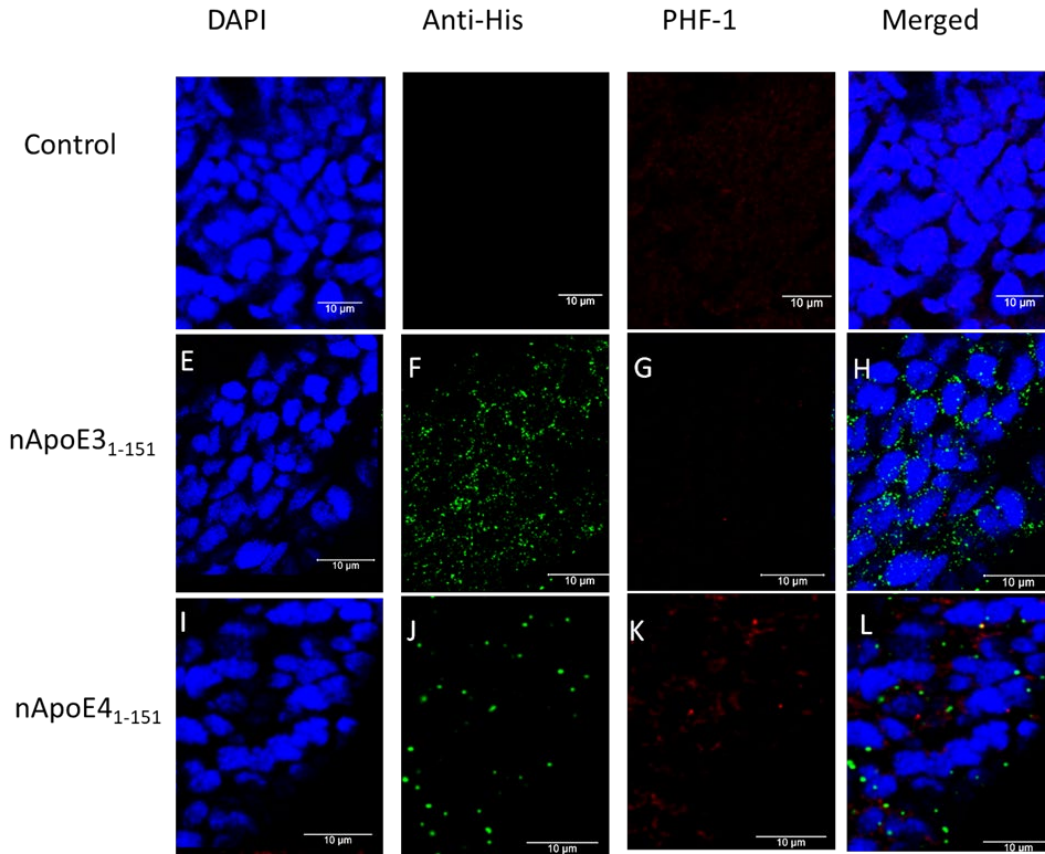
**Figure 4. Measurements of LDH and apoptosis indicate a cytotoxic role for nApoE41-151 (A-C).**

(A) The Mosaic Plot depicts mortality based on a lack of heartbeat and response to physical stimuli following exogenous treatment of 48hpf zebrafish embryos with either 25  $\mu\text{g}/\text{mL}$  nApoE3<sub>1-151</sub> or nApoE4<sub>1-151</sub> for 24 hours. The blue filled region of the bar graph designates 25  $\mu\text{g}/\text{mL}$  treatment of nApoE4<sub>1-151</sub> which led to a significant portion of the embryos being designated as dead. The red dotted portion of the bar graphs indicates less than expected were alive ( $p=1.17\text{e-}13$ ). All blank cells indicate the sample group followed the estimated trend. Data indicated significant mortality for only the nApoE4<sub>1-151</sub> group. N=3 independent experiments, 15 embryos/treatment. (B) Represents the results of LDH analysis utilizing 50  $\mu\text{g}/\text{mL}$  concentrations for both E3 and E4 fragments. Data established trend but not significance ( $p>0.05$ ). Error bars show  $\pm$ -SEM. (C) Results from western blot with an activated caspase-3 antibody. The presence of the two small domains of caspase-3 indicates activation of apoptotic pathways within nApoE4<sub>1-151</sub> treated samples. Coomassie blue stained transfer gel shown below to verify protein loading.



**Figure 5. Exogenous treatment of zebrafish embryos with amino-terminal fragments of nApoE4<sub>1-151</sub> leads to nuclear localization. (A-D).**

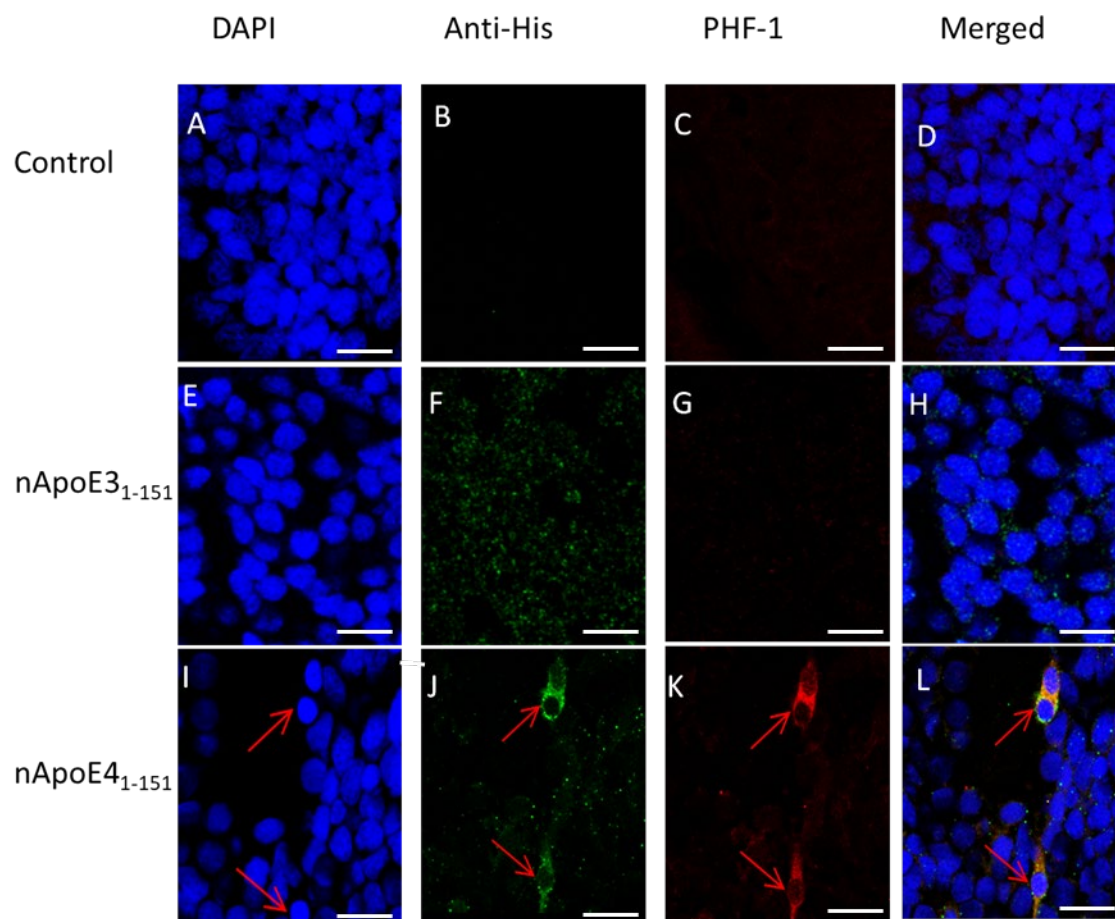
Representative images from confocal immunofluorescence in 5mm paraffin embedded sections of non-treated control 48hpf zebrafish embryos that were stained with DAPI (A), NeuN (1:50). (B), anti-His antibody (1:500) (C), and the merged image in Panel (D). There was no detection of any nApoE<sub>1-151</sub> fragments in untreated control neuronal cells as indicated by the lack of labeling in Panel C. **(E-H)** Identical to Panels A-D with the exception that embryos were exogenously treated for 24 hours with 25  $\mu\text{g/ml}$  of nApoE3<sub>1-151</sub>. Perinuclear localization of nApoE3<sub>1-151</sub> was evident (**Panel G and H, arrows**) under these conditions. **(I-L)** Parallel experiments as in Panels E-H with the exception that zebrafish embryos were treated exogenously for 24 hours with 25  $\mu\text{g/mL}$  of nApoE4<sub>1-151</sub>. In this case, strong nuclear localization of nApoE4<sub>1-151</sub> was evident within neuronal cells (**Panels K and L, arrows**). For both fragments, staining appears punctate and co-localized with NeuN and DAPI. All images were captured within the area of the cerebellum and fourth ventricle. Data are representative of three independent experiments. All scale bars represent 10  $\mu\text{m}$ .



**Figure 6. Tau Pathology present after treatment with exogenous nApoE4<sub>1-151</sub> Fragment in 48hpf zebrafish brain. (A-D).**

Representative 40x images from confocal immunofluorescence in 5 $\mu$ m paraffin embedded sections of non-treated control 48hpf zebrafish embryos that were stained with DAPI, PHF-1 (1:250), and Anti-6x His Tag antibody to detect nApoE4<sub>1-151</sub> (1:500). **(E-H)**: Parallel experiments as in Panels A-C with the exception that zebrafish embryos were treated exogenously for 24 hours with 25  $\mu$ g/mL of nApoE4<sub>1-151</sub>. Little to no PHF-1 detected at 48hpf in nApoE3<sub>1-151</sub>. **(I-L)**: Parallel experiments as in Panels A-C with the exception that zebrafish embryos were treated exogenously for 24 hours with 25  $\mu$ g/mL of nApoE4<sub>1-151</sub>. Light detection of PHF-1 compared to control and nApoE3<sub>1-151</sub> sections. All scale bars represent 10  $\mu$ m.





**Figure 7. Tau Pathology present after treatment with exogenous nApoE41-151 Fragment in 72hpf zebrafish brain. (A-D).**

Representative 40x zoomed images from confocal immunofluorescence in 5 $\mu$ m paraffin embedded sections of non-treated control 72hpf zebrafish embryos that were stained with DAPI, PHF-1 (1:250), and Anti-6x-His- Tag antibody to detect nApoE4<sub>1-151</sub> (1:500). **(E-H)**: Parallel experiments as in Panels A-C with the exception that zebrafish embryos were treated exogenously for 24 hours with 25  $\mu$ g/mL of nApoE3<sub>1-151</sub> then given 24 hours in clean media before using for experiment at 72hpf. Presence of PHF-1 staining overlap with nApoE3<sub>1-151</sub> noted with red arrow, PHF-1 staining does not appear to change structure of protrusions from nuclei (E-H). **(I-L)**: Parallel experiments as in Panels A-C with the exception that zebrafish embryos were treated exogenously for 24 hours with 25 $\mu$ g/mL of nApoE4<sub>1-151</sub> then given 24 hours in clean media before using for experiment at 72hpf. Presence of AD-like tau pathology noted with red arrows; PHF-1 labeling that overlaps with nApoE4<sub>1-151</sub> appears aggregated compared to staining in nApoE3<sub>1-151</sub> (I-L).

All scale bars represent 10  $\mu$ m.

## CHAPTER FOUR: BEHAVIORAL EFFECTS

### Overview

In the fourth chapter of this thesis, the focus is centered on the potential behavioral deficits following treatment of zebrafish with nApoE4<sub>1-151</sub>. Behavioral effects in this thesis provides relevant context to the molecular and morphological data provided in previous chapters. Embryonic motor behavior begins around 24-27 hours post-fertilization with spontaneous tail twitching with response to stimuli beginning shortly after (Saint-Amant & Drapeau, 2000). Initial twitches and response to stimuli prior to the hatching period (<48hpf) have been shown to exist within a rostral spinal cord loop (Pietri et al., 2009; Saint-Amant & Drapeau, 2000). The development of a hindbrain integrated circuit controlling spontaneous tail movement and the ability to respond rapidly to touch stimulus occurs after Mauthner cell maturity around the time of hatching (Eaton et al., 1977). Assessing the behavior of zebrafish in larvae (post-hatching) is therefore more aligned with mature motor circuitry in zebrafish.

My thesis employed modifications of previously reported methods in order to assess whether nApoE4<sub>1-151</sub> treatment impacts the presence of either the spontaneous tail flick behavior referred to herein as the tail flick test (TFT) or touch-response test referred to herein as the touch-evoked movement response (TEMR). The TFT experimental design utilized in the present study is a modification on one employed by Roberts et al. (Roberts et al., 2020). The TEMR design was based on the described behavior in (Kalueff et al., 2013). TFT and TEMR tests utilized larvae approximately at 72 hpf +/-2 hours to align data with the hindbrain associated circuit. Both tests are valuable in determining

proper development of motor behaviors. Our design would be aligned with a predicted hypoactive response, meaning we hypothesize that nApoE4<sub>1-151</sub> treated samples will be the lowest performing group in both assays.

## **Materials and Methods**

### Tail Flick Behavioral Test

Larvae were acclimated to the testing area for 2 minutes prior to experimentation. Five-minute videos were taken of each larvae using a Motic MGT 101 Moticam recording device with an LED-60T-B light ring. Videos were recorded down each treatment group column, then across well rows in a 96-well petri dish. Immediately following testing, the samples were euthanized using IACUC and University Guidelines, preserved in 4% PFA/PBT, then stored in 100% ethanol at -20°C. During each recording individual larva were documented using a numerical code to designate treatment groups for a single-blind procedure, in which one researcher recorded and encoded video names for treatment and a second researcher analyzed coded videos. Scoring was completed by examining videos while documenting the number of tail flicks in total for each larva over a 5-minute span, then dividing the total by 5 (Tail Flicks per Minute). A single tail flick was determined by counting the number of times each larva bent their tail away from center and returned to the center axis. Samples were prepared by averaging 5 tail flicks per replicate over the course of 5 replicates for trial one using nApoE3<sub>1-151</sub> 10 µg/mL (final concentration) and nApoE4<sub>1-151</sub> at a final concentration of 10 µg/mL. Ten micrograms per milliliter was the initial concentration we chose to identify whether a reduced treatment level (<50% of a sublethal concentration) would evoke behavioral responses prior without a decrease in survivability; 10 replicates for trial two using

nApoE3<sub>1-151</sub> 25 µg/mL and nApoE4<sub>1-151</sub> 25 µg/mL (final concentrations). Concentrations were raised in trial 2 to align data with other experimental outcomes as opposed to visualizing a minimum treatment effect. Data analyzed for each trial represent the averaged results for each collection date. Data was analyzed through two-way ANOVA modeling with three treatment groups (Control, nApoE3<sub>1-151</sub>, and nApoE4<sub>1-151</sub>) in R statistical software. The ANOVA model was assessed for assumptions after creation of model in R.

#### Touch Evoked Movement Response Assay

Individual larvae at 72hpf were moved to a 14x14 mm round glass bottom petri dish filled with E3 Media 2 minutes prior to testing for acclimation under light conditions for testing. Two-minute videos were recorded on Motic MGT 101 Moticam recording device with an LED-60T-B light ring. After the start of the recording at time (T=0), embryos were tapped lightly with a blunt probe every 15 seconds to allow the media to settle and original movement to terminate. Directly following testing, larvae were euthanized using IACUC and University Guidelines, preserved in 4% PFA/PBT, then stored in 100% ethanol at -20°C. Videos were analyzed in Noldus Behavioral Software version 15.0. Criteria for scoring was based on the number of responses following the evoked stimulus. Data was grouped by treatment and analyzed in R statistical software. Data was assessed for normality and variance. The number of responses to the evoked stimulus was analyzed using One-Way ANOVA.

## Results

### Tail Flick Test Assay

In trial 1 of TFT (**Figure 8A**), nApoE4<sub>1-151</sub> performed the least number of tail flicks per group with >50% reduction from untreated controls. Treatment of zebrafish larvae with nApoE3<sub>1-151</sub> performed similarly to controls. No difference was significant across any group ( $F(2,12) = 2.49, p=0.125$ ). Trial 1 was repeated due to numerous confounding variables explained in the conclusion section.

Trial 2 of TFT (**Figure 8B**) spontaneous tail flicks were <1 per minute for all treatment groups. nApoE3<sub>1-151</sub> outperformed tail flick median of all other groups, with the nApoE4<sub>1-151</sub> treated cohorts were again at the lowest performing group. No significance was detected between any groups compared ( $F(2,27)=1.24, p=0.305$ ).

### Touch-Evoked Movement Response Assay

For the TEMR, control groups and nApoE3<sub>1-151</sub> treated groups responded to 90% of the stimulations applied. nApoE4<sub>1-151</sub> treated samples responded to fewer than 50% of stimulations. Significance was not achieved groups ( $F(12)=1.482, p=0.266$ ). Results are shown in **Figure 9**.

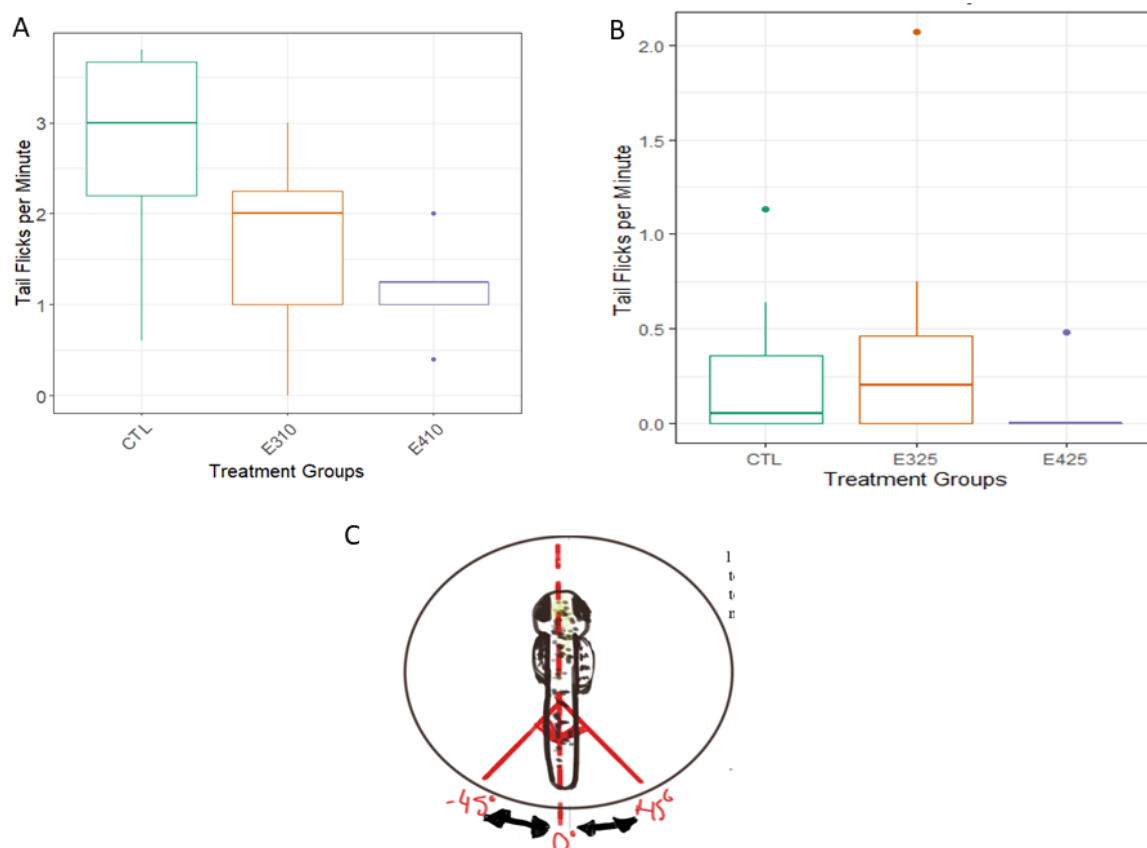
## Conclusions

The first TFT assay appeared initially to indicate strong spontaneous tail flick activity in controls and nApoE3<sub>1-151</sub> treated samples whereas a reduced response was found in nApoE4<sub>1-151</sub> treated samples (**Figure 8A**). The data from this trial, however, had large variation within groups. Some of the pitfalls of this first TFT trial were the recording area for this study. The area itself was a shared research space that did not have enclosed spaces to perform sensitive experiments. As such, there were external

disturbances throughout the area during recordings which potentially influenced the results by adding unintentional stimulation to the testing zebrafish. The TFT assay was repeated due to several those confounding variables (**Figure 8A**). TFT trial 2 (**Figure 8B**) cohorts demonstrated minimal spontaneous tail flick behavior in a controlled environment. The lack of response in the trial, while counterintuitive to our original hypothesis, indicates there is limited motor initiation in our 72hpf larvae in an unstimulated environment.

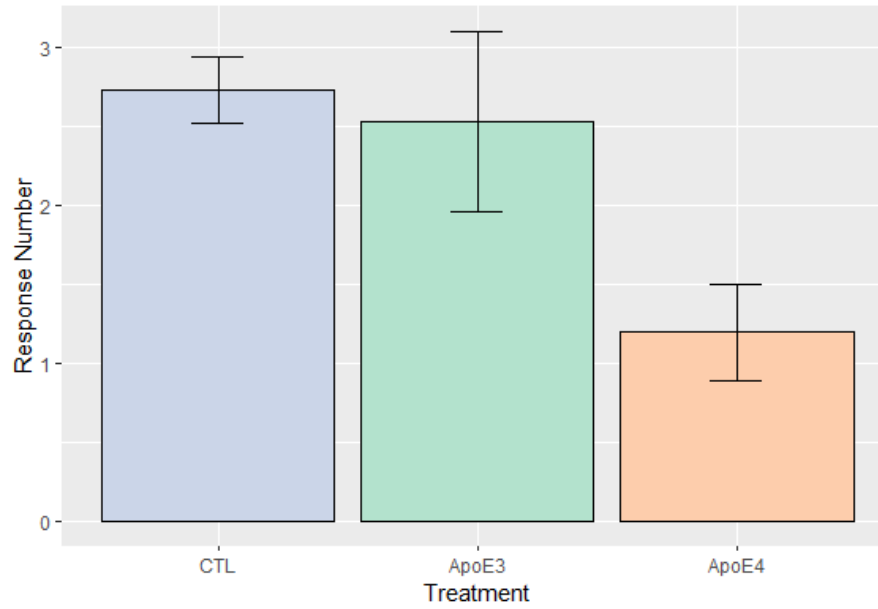
Despite the lack of statistical significance in the data for the TEMR, the presence of a consistent trend remains with untreated controls responding to over 90% of the stimuli on average while nApoE3<sub>1-151</sub> treated larvae responded to >80%, and nApoE4<sub>1-151</sub> responded to fewer than 50% of the stimulations. The nApoE4<sub>1-151</sub> -treated cohorts remained the lowest scoring treatment category for TEMR. There was a 50% reduction in response rate from nApoE4<sub>1-151</sub> from the control group. Data while following a trend for motor impairment following treatment with nApoE4<sub>1-151</sub> was not statistically significant from untreated controls ( $F(2,12)=1.482$ ,  $p=0.266$ ). This experiment had its own pitfalls such as the lack of using a structured testing to test if any difference could be observed from response to either a left- or right-side tail stimulus. Additionally, the testing 14x14mm petri dish had moved in several videos during testing which required a prompt reset of the dish back into focus. The latter of the two was better controlled for in video analyses as the reviewer could exclude responses that happened during the resetting process. Lastly, there was no random sampling applied to the testing method, controls were analyzed first, then nApoE3<sub>1-151</sub>, followed by nApoE4<sub>1-151</sub> for every trial. These factors likely contributed to variation for this test.

## Figures



**Figure 8. TFT trials finds no difference in unstimulated muscle twitches between treatment groups (A-C).**

(A) TFT trial 1 results were inconclusive with no difference detectable among any groups tested despite a declining trend in data ( $F(2,12) = 2.49, p=0.125$ ). Groups for Control, ApoE3<sub>1-151</sub> 10µg/ml (E310), and ApoE4<sub>1-151</sub> 10µg/ml (E410) were assessed via video monitoring to determine number of tail flicks per minute that were then averaged per group for each trial. Data are representative of N=5 trials, for a total of 25 embryos per group. The median is depicted in boxplot with quantiles. Potential outliers are shown as dots (B) Trial 2 reported limited spontaneous tail flick activation from every group with no difference detectable between groups ( $F(2,27)=1.24, p=0.305$ ). (C) Diagram visualizing the test, figure in center is larva in well plate from the perspective of the recording microscope. Red dotted line is the inferred midline of the larva from the sagittal plane. The solid lines were used as a reference for video scorers to grade response as a tail flick. Tail flicks were expected to fall between 45°.



**Figure 9. Touch-Evoked Movement Response outcomes lack significance but identify a clear decreasing trend through treatment groups.**

ApoE4 treatment groups on average responded 50% less than Controls ( $F(12)=1.482$ ,  $p=0.266$ ). Controls had a 90% response rate to the stimulus, whereas nApoE4<sub>1-151</sub> responded to fewer than 50% of invoked stimulus.



## CHAPTER FIVE: DISCUSSION

Mechanistic research into the pathophysiological relationship between harboring the *APOE4* allele and the development of late-onset AD have been on-going for decades. Prior research from our lab supports the hypothesis that ApoE4 fragmentation via MMP-9 may contribute to AD pathology and inflammation (Love et al., 2017). Other studies have also shown neurotoxic and pro-inflammatory responses to the fragmentation of ApoE4 (Dafnis et al., 2012; Tolar et al., 1997; Zhou et al., 2006). The research provided in this thesis brings *in vivo* relevance and expands on our previous studies utilizing transformed BV2 microglial cells to understand nApoE4<sub>1-151</sub> in an organismal context.

Using exogenously applied nApoE4<sub>1-151</sub> to assess morphological effects in zebrafish, our results indicate a potential interaction between nApoE4<sub>1-151</sub> with nervous system, cardiovascular, and pigmentation development. The nervous system was visibly impacted by the lack of hindbrain folding that is typical in 48hpf zebrafish along the cerebellar primordium Figure 3C. Additionally, exogenous nApoE4<sub>1-151</sub> treatments at both a low (25µg/mL) and high (50µg/mL) concentrations produced significant differences from controls in terms of developmental abnormalities and reduced heart rates. The morphological results of enlargement of hearts following nApoE4<sub>1-151</sub> treatment supports the link between inheritance of *APOE4* and an increased risk of cardiovascular disease (Carlos Lahoz, 2001). Our immunohistochemical results may shed light on our heart rate effects in nApoE4<sub>1-151</sub>. Nuclear staining in neurons labeled with NeuN have been observed in the hindbrain region around the medulla oblongata (MO) which regulates heart rate. Our research supports the likelihood that nApoE4<sub>1-151</sub>

contributes to a cytotoxic environment through upregulation of key apoptotic regulators such as caspase-3. These data support the hypothesis that nApoE4<sub>1-151</sub> may destabilize the hindbrain networks during the incubation period. These results open an avenue for further research into whether nApoE4<sub>1-151</sub> directly impacts cardiovascular tissue or whether there is a downstream effect from the presence of nApoE4<sub>1-151</sub> in the hindbrain.

Additionally, increased detection of nApoE4<sub>1-151</sub> compared to controls within the hindbrain region could be an avenue for the effects observed in the TEMR assay. The touch escape response and spontaneous tail flicks are both proposed to be regulated by the Mauthner cells located in the zebrafish hindbrain (Eaton et al., 1977; Liu & Fetcho, 1999). Treatment of zebrafish larvae with nApoE4<sub>1-151</sub> led to less than half of the stimulation attempts whereas control responded to over 90% and nApoE3<sub>1-151</sub> responded to over 80%. Future experiments for this study would be to evaluate at what stage in this behavior does nApoE4<sub>1-151</sub> interfere: initiation or execution of the behavioral response. Initiation of the response would imply the sensation of the stimulus was never received through the rohon-beard cells or the dorsal root ganglia which have been shown to share the responsibility of tactile sensation during the 72hpf period (Pietri et al., 2009; Saint-Amant & Drapeau, 2000).

Another important result from these studies was the increased presence of PHF-1 labeling in nApoE4<sub>1-151</sub> treated samples that resembles AD-like tau pathology beginning at 48hpf and increasing at 72hpf (as seen in **Figures 6 and 7**). These findings support that nApoE4<sub>1-151</sub> may promote tau pathology, a hallmark feature seen in human AD pathology (Lin et al., 2018). The observed tau pathology can lead to disruptions in axonal health which in turn, can have deleterious effects on neuronal signaling and axonal transport

(Forner et al., 2017; Kowall & Kosik, 1987). These results help to clarify that treatment with nApoE4<sub>1-151</sub> leads to a dysfunctional, disease state. Future steps for this aspect of my thesis include pursuing a transgenic model that carries an inserted nApoE4<sub>1-151</sub> insertion to allow continuous expression of the protein fragment. A transgenic model will help to provide a more consistent model for nApoE4<sub>1-151</sub> effects that are expressed consistently throughout embryogenesis and into adulthood as opposed to our 24-hour incubation period. We expect to pursue more behavioral testing in the future for locomotion and memory for mutant nApoE4<sub>1-151</sub> compared to wild-type controls.

Taken together, the results of my thesis stand as a proof-of-concept that extends the results of the prior *in vitro* experiments from our lab to an *in vivo* vertebrate model system. This thesis also fills gaps within the scientific literature as to how an amino-terminal ApoE4 fragment can influence the progression of embryogenesis, and that ApoE4 can influence the development of the cardiovascular system.

In conclusion, this work supports the hypothesis that the presence of amino-terminal ApoE4 fragments can negatively impact developmental outcomes, promote cytotoxicity, and stimulate a toxic gain-of-function resulting in an AD-like tau pathology.

## REFERENCES

- Association, A. s. (2019). 2019 Alzheimer's disease facts and figures. *Alzheimer's & Dementia*, *15*(3), 321-387.  
<https://doi.org/https://doi.org/10.1016/j.jalz.2019.01.010>
- Babin, P. J., Goizet, C., & Raldúa, D. (2014). Zebrafish models of human motor neuron diseases: Advantages and limitations. *Progress in Neurobiology*, *118*, 36-58.  
<https://doi.org/10.1016/j.pneurobio.2014.03.001>
- Beckers, A., Van Dyck, A., Bollaerts, I., Van houcke, J., Lefevre, E., Andries, L., Agostinone, J., Van Hove, I., Di Polo, A., Lemmens, K., & Moons, L. (2019). An Antagonistic Axon-Dendrite Interplay Enables Efficient Neuronal Repair in the Adult Zebrafish Central Nervous System. *Molecular Neurobiology*, *56*(5), 3175-3192. <https://doi.org/10.1007/s12035-018-1292-5>
- Buttini, M., Orth, M., Bellosta, S., Akeefe, H., Pitas, R. E., Wyss-Coray, T., Mucke, L., & Mahley, R. W. (1999). Expression of human apolipoprotein E3 or E4 in the brains of Apoe(-/-) mice: Isoform-specific effects on neurodegeneration. *Journal of Neuroscience*, *19*(12), 4867-4880. <https://doi.org/10.1523/jneurosci.19-12-04867.1999>
- Carlos Lahoz, E. J. S., L.Adrienne Cupples, Peter W.F. Wilson, Daniel Levy, Doreen Osgood, Stefanos Parpos, Juan Pedro-Botet, Jennifer A. Daly, Jose M. Ordovas,. (2001). Apolipoprotein E genotype and cardiovascular disease in the Framingham Heart Study, . *Atherosclerosis*, *154*(3), 529-537.  
[https://doi.org/https://doi.org/10.1016/S0021-9150\(00\)00570-0](https://doi.org/https://doi.org/10.1016/S0021-9150(00)00570-0)
- Cho, H. S., Hyman, B. T., Greenberg, S. M., & Rebeck, G. W. (2001). Quantitation of apoE domains in Alzheimer disease brain suggests a role for apoE in Abeta aggregation. *J Neuropathol Exp Neurol*, *60*(4), 342-349.  
<https://doi.org/10.1093/jnen/60.4.342>

- Dafnis, I., Tzinia, A. K., Tsilibary, E. C., Zannis, V. I., & Chroni, A. (2012). An apolipoprotein E4 fragment affects matrix metalloproteinase 9, tissue inhibitor of metalloproteinase 1 and cytokine levels in brain cell lines. *Neuroscience*, *210*, 21-32. <https://doi.org/10.1016/j.neuroscience.2012.03.013>
- DeTure, M. A., & Dickson, D. W. (2019). The neuropathological diagnosis of Alzheimer's disease. *Mol Neurodegener*, *14*(1), 32. <https://doi.org/10.1186/s13024-019-0333-5>
- Diamantino, T. C., Almeida, E., Soares, A. M., & Guilhermino, L. (2001). Lactate dehydrogenase activity as an effect criterion in toxicity tests with *Daphnia magna* straus. *Chemosphere*, *45*(4-5), 553-560. [https://doi.org/10.1016/s0045-6535\(01\)00029-7](https://doi.org/10.1016/s0045-6535(01)00029-7)
- Eaton, R. C., Farley, R. D., Kimmel, C. B., & Schabtach, E. (1977). Functional development in the Mauthner cell system of embryos and larvae of the zebra fish. *J Neurobiol*, *8*(2), 151-172. <https://doi.org/10.1002/neu.480080207>
- Forner, S., Baglietto-Vargas, D., Martini, A. C., Trujillo-Estrada, L., & LaFerla, F. M. (2017). Synaptic Impairment in Alzheimer's Disease: A Dysregulated Symphony. *Trends Neurosci*, *40*(6), 347-357. <https://doi.org/10.1016/j.tins.2017.04.002>
- Goldstein, J. L., & Brown, M. S. (1976). The LDL pathway in human fibroblasts: a receptor-mediated mechanism for the regulation of cholesterol metabolism. *Curr Top Cell Regul*, *11*, 147-181. <https://doi.org/10.1016/b978-0-12-152811-9.50011-0>
- Gottschall, P. E., & Deb, S. (1996). Regulation of matrix metalloproteinase expressions in astrocytes, microglia and neurons. *Neuroimmunomodulation*, *3*(2-3), 69-75. <https://doi.org/10.1159/000097229>

- Harris, F. M., Brecht, W. J., Xu, Q., Tesseur, I., Kekonius, L., Wyss-Coray, T., Fish, J. D., Masliah, E., Hopkins, P. C., Searce-Levie, K., Weisgraber, K. H., Mucke, L., Mahley, R. W., & Huang, Y. (2003). Carboxyl-terminal-truncated apolipoprotein E4 causes Alzheimer's disease-like neurodegeneration and behavioral deficits in transgenic mice. *Proceedings of the National Academy of Sciences*, *100*(19), 10966-10971. <https://doi.org/10.1073/pnas.1434398100>
- He, Z., Guo, J. L., McBride, J. D., Narasimhan, S., Kim, H., Changolkar, L., Zhang, B., Gathagan, R. J., Yue, C., Dengler, C., Stieber, A., Nitla, M., Coulter, D. A., Abel, T., Brunden, K. R., Trojanowski, J. Q., & Lee, V. M. (2018). Amyloid- $\beta$  plaques enhance Alzheimer's brain tau-seeded pathologies by facilitating neuritic plaque tau aggregation. *Nat Med*, *24*(1), 29-38. <https://doi.org/10.1038/nm.4443>
- Horzmann, K. A., & Freeman, J. L. (2018). Making Waves: New Developments in Toxicology With the Zebrafish. *Toxicol Sci*, *163*(1), 5-12. <https://doi.org/10.1093/toxsci/kfy044>
- Howe, K. L., Achuthan, P., Allen, J., Allen, J., Alvarez-Jarreta, J., Amode, M. R., Armean, I. M., Azov, A. G., Bennett, R., Bhai, J., Billis, K., Boddu, S., Charkhchi, M., Cummins, C., Da Rin Fioretto, L., Davidson, C., Dodiya, K., El Houdaigui, B., Fatima, R., . . . Flicek, P. (2020). Ensembl 2021. *Nucleic Acids Research*, *49*(D1), D884-D891. <https://doi.org/10.1093/nar/gkaa942>
- Innerarity, T. L., & Mahley, R. W. (1978). Enhanced binding by cultured human fibroblasts of apo-E-containing lipoproteins as compared with low density lipoproteins. *Biochemistry*, *17*(8), 1440-1447. <https://doi.org/10.1021/bi00601a013>
- Kalueff, A. V., Gebhardt, M., Stewart, A. M., Cachat, J. M., Brimmer, M., Chawla, J. S., Craddock, C., Kyzar, E. J., Roth, A., Landsman, S., Gaikwad, S., Robinson, K., Baatrup, E., Tierney, K., Shamchuk, A., Norton, W., Miller, N., Nicolson, T., Braubach, O., . . . Schneider, H. (2013). Towards a comprehensive catalog of zebrafish behavior 1.0 and beyond. *Zebrafish*, *10*(1), 70-86. <https://doi.org/10.1089/zeb.2012.0861>

- Kimmel, C. B., Ballard, W. W., Kimmel, S. R., Ullmann, B., & Schilling, T. F. (1995). Stages of embryonic development of the zebrafish. *Developmental Dynamics*, 203(3), 253-310. <https://doi.org/10.1002/aja.1002030302>
- Kowall, N. W., & Kosik, K. S. (1987). Axonal disruption and aberrant localization of tau protein characterize the neuropil pathology of Alzheimer's disease. *Ann Neurol*, 22(5), 639-643. <https://doi.org/10.1002/ana.410220514>
- Lin, Y. T., Seo, J., Gao, F., Feldman, H. M., Wen, H. L., Penney, J., Cam, H. P., Gjoneska, E., Raja, W. K., Cheng, J., Rueda, R., Kritskiy, O., Abdurrob, F., Peng, Z., Milo, B., Yu, C. J., Elmsaouri, S., Dey, D., Ko, T., . . . Tsai, L. H. (2018). APOE4 Causes Widespread Molecular and Cellular Alterations Associated with Alzheimer's Disease Phenotypes in Human iPSC-Derived Brain Cell Types. *Neuron*, 98(6), 1141-1154.e1147. <https://doi.org/10.1016/j.neuron.2018.05.008>
- Liu, K. S., & Fetcho, J. R. (1999). Laser ablations reveal functional relationships of segmental hindbrain neurons in zebrafish. *Neuron*, 23(2), 325-335. [https://doi.org/10.1016/s0896-6273\(00\)80783-7](https://doi.org/10.1016/s0896-6273(00)80783-7)
- Lossi, L., Castagna, C., & Merighi, A. (2018). Caspase-3 Mediated Cell Death in the Normal Development of the Mammalian Cerebellum. *Int J Mol Sci*, 19(12). <https://doi.org/10.3390/ijms19123999>
- Love, J. E., Day, R. J., Gause, J. W., Brown, R. J., Pu, X., Theis, D. I., Caraway, C. A., Poon, W. W., Rahman, A. A., Morrison, B. E., & Rohn, T. T. (2017). Nuclear uptake of an amino-terminal fragment of apolipoprotein E4 promotes cell death and localizes within microglia of the Alzheimer's disease brain. *Int J Physiol Pathophysiol Pharmacol*, 9(2), 40-57. <https://www.ncbi.nlm.nih.gov/pubmed/28533891>
- Lungu-Mitea, S., Vogs, C., Carlsson, G., Montag, M., Frieberg, K., Oskarsson, A., & Lundqvist, J. (2021). Modeling Bioavailable Concentrations in Zebrafish Cell Lines and Embryos Increases the Correlation of Toxicity Potencies across Test Systems. *Environ Sci Technol*, 55(1), 447-457. <https://doi.org/10.1021/acs.est.0c04872>

- Maharajan, K., Muthulakshmi, S., Nataraj, B., Ramesh, M., & Kadirvelu, K. (2018). Toxicity assessment of pyriproxyfen in vertebrate model zebrafish embryos (*Danio rerio*): A multi biomarker study. *Aquatic Toxicology*, *196*(February), 132-145. <https://doi.org/10.1016/j.aquatox.2018.01.010>
- Mahley, R. W. (2016). Central Nervous System Lipoproteins: ApoE and Regulation of Cholesterol Metabolism. *Arterioscler Thromb Vasc Biol*, *36*(7), 1305-1315. <https://doi.org/10.1161/ATVBAHA.116.307023>
- Martins, I. J., Hone, E., Foster, J. K., Sünram-Lea, S. I., Gnjec, A., Fuller, S. J., Nolan, D., Gandy, S. E., & Martins, R. N. (2006). Apolipoprotein E, cholesterol metabolism, diabetes, and the convergence of risk factors for Alzheimer's disease and cardiovascular disease. *Molecular Psychiatry*, *11*(8), 721-736. <https://doi.org/10.1038/sj.mp.4001854>
- Munoz, S. S., Li, H., Ruberu, K., Chu, Q., Saghatelian, A., Ooi, L., & Garner, B. (2018). The serine protease HtrA1 contributes to the formation of an extracellular 25-kDa apolipoprotein E fragment that stimulates neuritogenesis. *J Biol Chem*, *293*(11), 4071-4084. <https://doi.org/10.1074/jbc.RA117.001278>
- Musa, A., Lehrach, H., & Russo, V. A. (2001). Distinct expression patterns of two zebrafish homologues of the human APP gene during embryonic development. *Dev Genes Evol*, *211*(11), 563-567. <https://doi.org/10.1007/s00427-001-0189-9>
- Narita, M., Holtzman, D. M., Fagan, A. M., LaDu, M. J., Yu, L., Han, X., Gross, R. W., Bu, G., & Schwartz, A. L. (2002). Cellular catabolism of lipid poor apolipoprotein E via cell surface LDL receptor-related protein. *J Biochem*, *132*(5), 743-749. <https://doi.org/10.1093/oxfordjournals.jbchem.a003282>
- Nesan, D., & Vijayan, M. M. (2012). Embryo exposure to elevated cortisol level leads to cardiac performance dysfunction in zebrafish. *Molecular and Cellular Endocrinology*, *363*(1-2), 85-91. <https://doi.org/10.1016/j.mce.2012.07.010>
- Pietri, T., Manalo, E., Ryan, J., Saint-Amant, L., & Washbourne, P. (2009). Glutamate drives the touch response through a rostral loop in the spinal cord of zebrafish embryos. *Dev Neurobiol*, *69*(12), 780-795. <https://doi.org/10.1002/dneu.20741>



- Pollock, T. B., Cholico, G. N., Isho, N. F., Day, R. J., Suresh, T., Stewart, E. S., McCarthy, M. M., & Rohn, T. T. (2020). Transcriptome Analyses in BV2 Microglial Cells Following Treatment With Amino-Terminal Fragments of Apolipoprotein E. *Front Aging Neurosci*, *12*, 256. <https://doi.org/10.3389/fnagi.2020.00256>
- Pollock, T. B., Mack, J. M., Day, R. J., Isho, N. F., Brown, R. J., Oxford, A. E., Morrison, B. E., Hayden, E. J., & Rohn, T. T. (2019). A Fragment of Apolipoprotein E4 Leads to the Downregulation of a CXorf56 Homologue, a Novel ER-Associated Protein, and Activation of BV2 Microglial Cells. *Oxid Med Cell Longev*, *2019*, 5123565. <https://doi.org/10.1155/2019/5123565>
- Portavella, M., Torres, B., & Salas, C. (2004). Avoidance response in goldfish: emotional and temporal involvement of medial and lateral telencephalic pallium. *J Neurosci*, *24*(9), 2335-2342. <https://doi.org/10.1523/jneurosci.4930-03.2004>
- Roberts, A. C., Alzagatiti, J. B., Ly, D. T., Chornak, J. M., Ma, Y., Razee, A., Zavradyan, G., Khan, U., Lewis, J., Natarajan, A., Baibussinov, A., Emtage, J., Komaranchath, M., Richards, J., Hoang, M., Alipio, J., Laurent, E., Kumar, A., Campbell, C. S., . . . Glanzman, D. L. (2020). Induction of Short-Term Sensitization by an Aversive Chemical Stimulus in Zebrafish Larvae. *eNeuro*, *7*(6). <https://doi.org/10.1523/ENEURO.0336-19.2020>
- Rohn, T. T., Catlin, L. W., Coonse, K. G., & Habig, J. W. (2012). Identification of an amino-terminal fragment of apolipoprotein E4 that localizes to neurofibrillary tangles of the Alzheimer's disease brain. *Brain Res*, *1475*, 106-115. <https://doi.org/10.1016/j.brainres.2012.08.003>
- Saint-Amant, L., & Drapeau, P. (2000). Motoneuron activity patterns related to the earliest behavior of the zebrafish embryo. *J Neurosci*, *20*(11), 3964-3972. <https://doi.org/10.1523/jneurosci.20-11-03964.2000>
- Schmidt, R., Strähle, U., & Scholpp, S. (2013). Neurogenesis in zebrafish - from embryo to adult. *Neural Development*, *8*(1), 1-13. <https://doi.org/10.1186/1749-8104-8-3>
- Scientific, T. Pierce\_LDH\_Cytotoxicity.

- Tolar, M., Marques, M. A., Harmony, J. A., & Crutcher, K. A. (1997). Neurotoxicity of the 22 kDa thrombin-cleavage fragment of apolipoprotein E and related synthetic peptides is receptor-mediated. *J Neurosci*, *17*(15), 5678-5686.  
<https://doi.org/10.1523/jneurosci.17-15-05678.1997>
- Vargas, R., Thorsteinsson, H., & Karlsson, K. A. (2012). Spontaneous neural activity of the anterodorsal lobe and entopeduncular nucleus in adult zebrafish: a putative homologue of hippocampal sharp waves. *Behav Brain Res*, *229*(1), 10-20.  
<https://doi.org/10.1016/j.bbr.2011.12.025>
- Weisgraber, K. H. (1994). Apolipoprotein E: structure-function relationships. *Adv Protein Chem*, *45*, 249-302. [https://doi.org/10.1016/s0065-3233\(08\)60642-7](https://doi.org/10.1016/s0065-3233(08)60642-7)
- Wilson, C., Wardell, M. R., Weisgraber, K. H., Mahley, R. W., & Agard, D. A. (1991). Three-dimensional structure of the LDL receptor-binding domain of human apolipoprotein E. *Science*, *252*(5014), 1817-1822.  
<https://doi.org/10.1126/science.2063194>
- Xie, C., Lund, E. G., Turley, S. D., Russell, D. W., & Dietschy, J. M. (2003). Quantitation of two pathways for cholesterol excretion from the brain in normal mice and mice with neurodegeneration. *Journal of Lipid Research*, *44*(9), 1780-1789. <https://doi.org/10.1194/jlr.m300164-jlr200>
- Zhou, W., Scott, S. A., Shelton, S. B., & Crutcher, K. A. (2006). Cathepsin D-mediated proteolysis of apolipoprotein E: possible role in Alzheimer's disease. *Neuroscience*, *143*(3), 689-701.  
<https://doi.org/10.1016/j.neuroscience.2006.08.019>